

## Neutrinoless double beta decay: interplay between nuclear matrix elements and neutrino exchange mechanisms

---

**Antonio Marrone,<sup>a,b,\*</sup> Eligio Lisi<sup>b</sup> and Newton Nath<sup>b</sup>**

<sup>a</sup>*Dipartimento Interateneo di Fisica “Michelangelo Merlin,”*

*Via Amendola 173, 70126 Bari, Italy*

<sup>b</sup>*Istituto Nazionale di Fisica Nucleare, Sezione di Bari, Via Orabona 4, 70126 Bari, Italy*

*E-mail:* [antonio.marrone@ba.infn.it](mailto:antonio.marrone@ba.infn.it)

We study neutrinoless double beta decay ( $0\nu\beta\beta$ ) mediated by non-interfering exchange of both light and heavy Majorana neutrinos, by taking into account recent calculations of nuclear matrix elements (NME) from various nuclear models. We put upper limits on the light and heavy neutrino contributions to  $0\nu\beta\beta$  decay, using data from current experiments (KamLAND-Zen, EXO, GERDA, MAJORANA, and CUORE), and also evaluates the potential signals at a significance level greater than  $3\sigma$  in future projects like nEXO, LEGEND, and CUPID.

*The European Physical Society Conference on High Energy Physics (EPS-HEP2023)  
21-25 August 2023  
Hamburg, Germany*

---

\*Speaker

## 1. Introduction

The pursuit of detecting  $0\nu\beta\beta$  in different isotopes, which involves the transformation of a nucleus  $(Z, A)$  into  $(Z + 2, A)$  while emitting two electrons, is a prominent endeavor in particle and nuclear physics. This process violates lepton number conservation by two units and holds the key to confirming that neutrinos are Majorana particles, regardless of the specific physics mechanisms involved. The primary mechanism considered in this work involves the exchange of three known light neutrinos, where the decay's half-life, denoted as  $T_i$  for a specific isotope  $i = (Z, A)$ , is governed by factors such as the phase-space factor  $G_i$ , the nuclear matrix element (NME)  $M_{\nu,i}$ , and the effective Majorana mass for light neutrinos  $m_\nu$ :

$$(T_i)^{-1} = S_i = G_i M_{\nu,i}^2 m_\nu^2 . \quad (1)$$

Alternative decay mechanisms can also be explored, especially those involving both light neutrinos ( $\nu_k$ ) and heavy Majorana neutrinos ( $N_h$ ) at the same time, which are important in scenarios beyond the Standard Model. In cases where these contributions do not interfere, the decay's half-life  $T_i$  and the signal  $S_i$  definitions can be extended to incorporate both light and heavy neutrino exchange:

$$(T_i)^{-1} = S_i = G_i \left( M_{\nu,i}^2 m_\nu^2 + M_{N,i}^2 m_N^2 \right) . \quad (2)$$

Our goal is to use experimental data from different isotopes to determine the values of  $m_\nu$  and  $m_N$ , provided that the heavy-to-light NME ratios are distinct for each isotope. If the NME ratios for heavy and light neutrino exchange differ among isotopes, a system of equations can be used to extract the unknown parameters  $m_\nu$  and  $m_N$ . If the NME ratios are similar, instead, the two mechanisms may become degenerate, making it challenging to distinguish them. Careful consideration of these ratios is essential for disentangling and confirming the presence of neutrinoless double beta

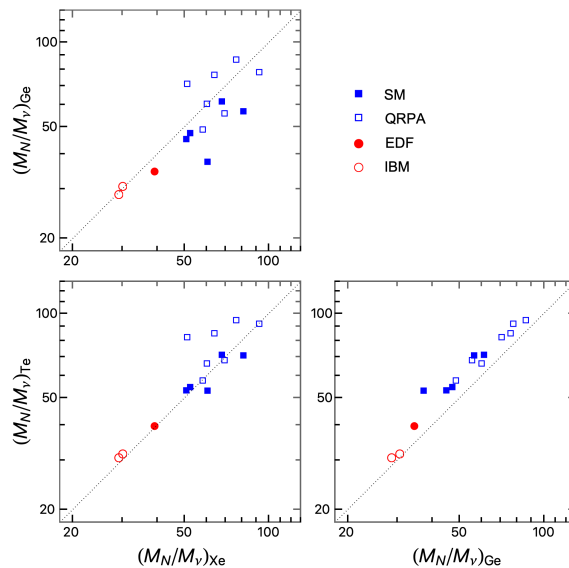


**Figure 1:** Scatter plot of  $M_{N,i}/M_{\nu,i}$  ratios for each pair of isotopes  $(i, j)$  among (Xe, Ge, Te). Each point refers to one of the fifteen NME sets in Table 1 of [1].

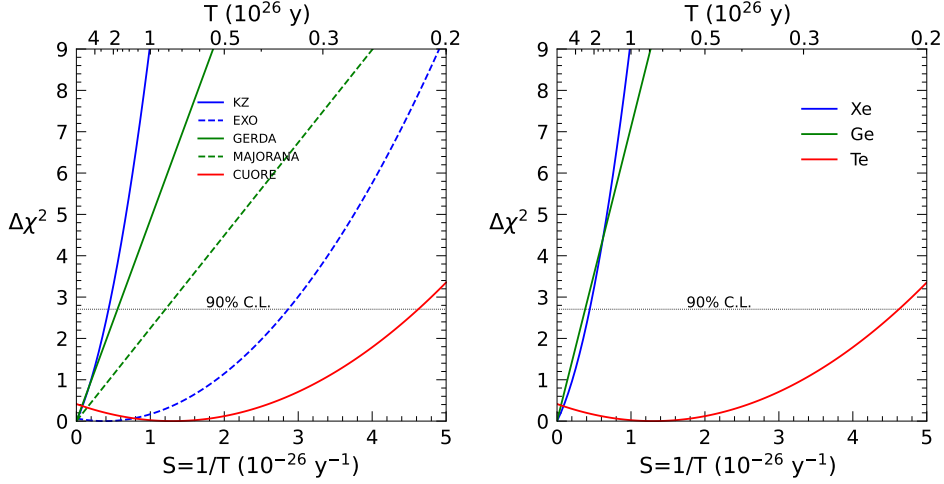


**Figure 2:**  $\Delta\chi^2$  functions in terms of the half-life  $T$  (top abscissa) and of the signal strength  $S = 1/T$  (bottom abscissa). Left and right panels: separate experiments and their combinations for the same isotope, respectively. Dotted horizontal lines intersect the curves at 90% C.L. See the text for details.

decay, especially in cases where interfering mechanisms are involved. In practice, there are several challenges in determining the parameters  $m_\nu$  and  $m_N$  in neutrinoless double beta decay: large uncertainties in nuclear matrix elements (NME) persist, and taking ratios does not always reduce them; the similarity of NME ratios across different isotopes complicates the analysis; current  $0\nu\beta\beta$  data show no clear signals, and future positive signals may have significant statistical uncertainties; multi-isotope measurements can either provide consistency checks or lead to unphysical solutions, depending on the assumed NME values and their ratios. Despite these challenges,  $0\nu\beta\beta$  decays involving light and heavy neutrinos remain a subject of great interest. Various theoretical models connecting these sectors may provide testable connections between the parameters  $m_\nu$  and  $m_N$ , and experimental efforts are ongoing to improve sensitivity and reduce uncertainties in NME calculations. In our study, we examine fifteen sets of Nuclear Matrix Elements (NMEs) that have been calculated over the past decade, as shown in Figure 1. Various theoretical methods and their variations were employed to derive these NMEs, including the nuclear shell model (SM), the quasi-particle random phase approximation (QRPA), the energy-density functional theory (EDF), and the interacting boson model (IBM). Notably, eight of these NME sets also encompass calculations for  $^{136}\text{Mo}$  using the QRPA, EDF, and IBM models.

## 2. Bounds from current data

The approach in this analysis is to associate to each experiment a  $\Delta\chi_i^2$  function, expressed as:

$$\Delta\chi_i^2(S_i) = a_i S_i^2 + b_i S_i + c_i, \quad (3)$$

where  $S_i$  represents the signal strength. We combine data from various experiments by summing their respective  $\Delta\chi^2$  functions. We derived constraints on the effective parameters  $m_\nu$  and  $m_N$  related to  $0\nu\beta\beta$  decay, by combining the  $\Delta\chi_i^2$  functions associated with the signals  $S_i$  in Xenon,

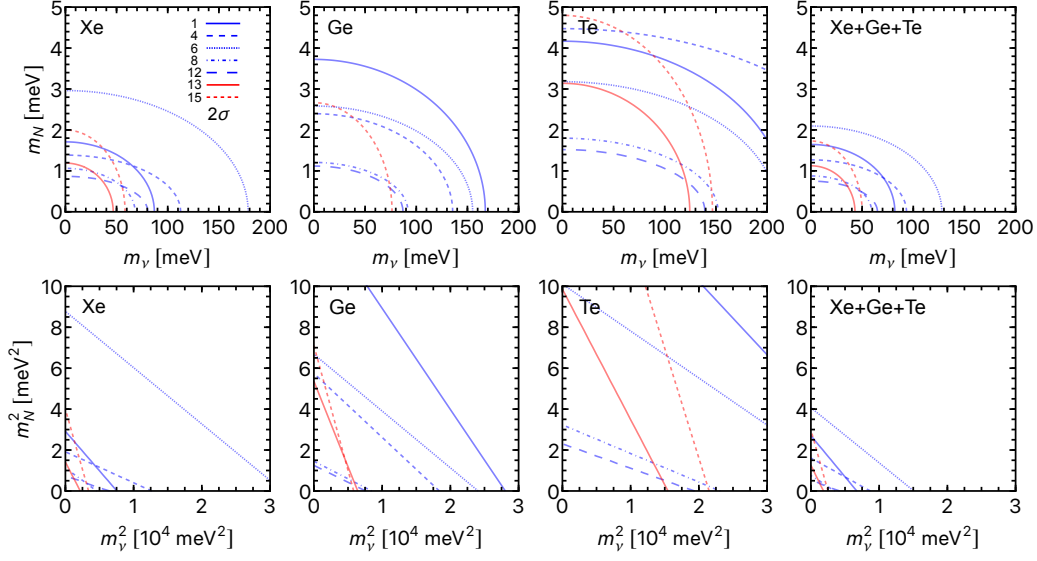


**Figure 3:** Joint upper bounds on the effective Majorana masses for the exchange of light neutrinos ( $m_\nu$ ) and heavy neutrinos ( $m_N$ ) from current Xe, Ge and Te data, under the assumption of non-interfering exchange, Eq. (2). All bounds are derived at the  $2\sigma$  confidence level.

Germanium, and Tellurium. Figure 3 illustrates the combined upper bounds on the effective Majorana mass parameters ( $m_\nu, m_N$ ), using data from current experiments. The regions below each curve represent the allowed parameter space at  $2\sigma$  ( $\Delta\chi^2 = 4$ ). For clarity, we have selected cases that represent relatively strong or weak bounds, considering seven different nuclear matrix element (NME) sets, among the ones listed in Table 1 of [1]. Lower panels in Figure 3 show the same bounds in terms of the squared variables ( $m_\nu^2, m_N^2$ ). The relationship between the effective mass parameters and the squared variables is linear in our analysis. For each NME set, the slope of the linear bound reflects the ratio of heavy neutrino mass to light neutrino mass for each isotope. The bounds for separate Xe, Ge, and Te isotopes are exactly linear, as the equations are linear in the squared variables. The combination of Xe, Ge, and Te data, while theoretically non-linear, is effectively close to linear in practice.

## 2.1 Future Projects

In this Section, we analyze examples of possible  $0\nu\beta\beta$  decay signals at  $> 3\sigma$  in future ton-scale projects. We discuss the reconstruction of hypothetical signals for fixed NME sets. We characterize a generic  $0\nu\beta\beta$  search as a counting experiment for a given exposure. In this counting experiment, we observe a total number of events, denoted as  $n$ , with respect to an average expectation of  $\mu$  events. The observed number  $n$  is the sum of the signal  $n_S$  and the background  $n_B$ . For our analysis, we use the Poissonian  $\chi^2$  function. In practical  $0\nu\beta\beta$  experiments, the estimation of background and signal event likelihoods can involve additional information, such as energy, time, and position characteristics. By appropriately choosing effective values for  $n_B$  for specific exposures, we can approximate the sensitivity to a generic signal  $n_S$ . We consider three sets of representative pairs for

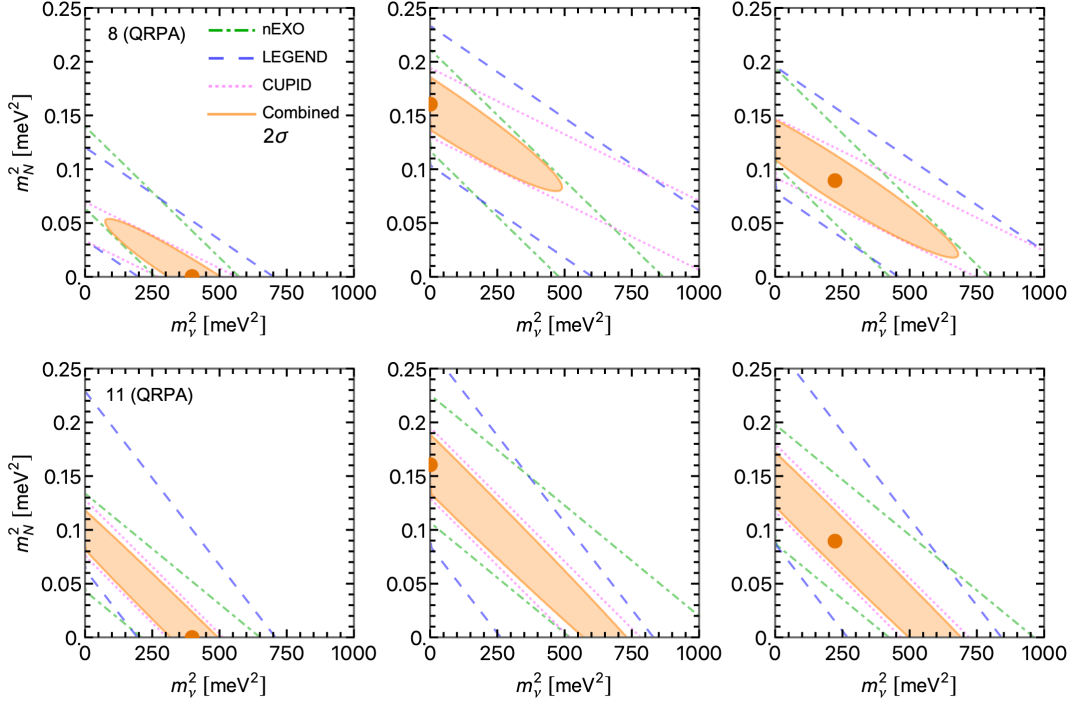


**Figure 4:** Fit to prospective data at  $2\sigma$  level. The upper and lower panels refer to the NME sets numbered as 8 and 11 in Table 1 of [1].

the true simulated effective Majorana masses, denoted as  $\bar{m}_\nu$ , and  $\bar{m}_N$ :

$$(\bar{m}_\nu, \bar{m}_N) = \begin{cases} (20, 0) \text{ meV} & \leftarrow \text{light } \nu_k \text{ only ,} \\ (0, 0.4) \text{ meV} & \leftarrow \text{heavy } N_h \text{ only ,} \\ (15, 0.3) \text{ meV} & \leftarrow \text{light } \nu_k + \text{heavy } N_h . \end{cases} \quad (4)$$

These values are small enough to satisfy the most stringent  $2\sigma$  upper bounds provided by current data while also being sufficiently high to yield a  $> 3\sigma$  signal, in each ton-scale experiment. The true signals are then fitted by test signals, both separately and in combination. We assume that the true and test NME sets are identical, as if they had no uncertainties. This assumption is relaxed in [1]. In the  $(m_\nu^2, m_N^2)$  plane,  $\chi^2$  isolines appear as slanted bands for separate isotopes. However, in multi-isotope combinations, they manifest as ellipses. The slopes of these bands are primarily governed by the  $M_{N,i}/M_{\nu,i}$  ratios, leading to variations in the overlap among them. The extent of the ellipses and the degree of degeneracy between the two  $0\nu\beta\beta$  mechanisms depend on the differences among these ratios. Smaller differences result in closer slopes and larger overlap, implying higher degeneracy between the two mechanisms. We selected four representative NME sets, numbered from 8 to 15 in Table 1 of [1]. These sets exhibit different characteristics in terms of  $M_{N,i}/M_{\nu,i}$  ratios: the two QRPA sets labeled as 8 and 11 have relatively high ratios  $M_{N,i}/M_{\nu,i}$ , the EDF set labeled as 13 provides intermediate values of the  $M_{N,i}/M_{\nu,i}$  ratios, and the IBM set numbered as 15 offers relatively low  $M_{N,i}/M_{\nu,i}$  values. It is worth noting that other NME sets yield qualitatively similar results. Figures 4 and 5 depict the  $2\sigma$  constraints from ton-scale experiments. These results

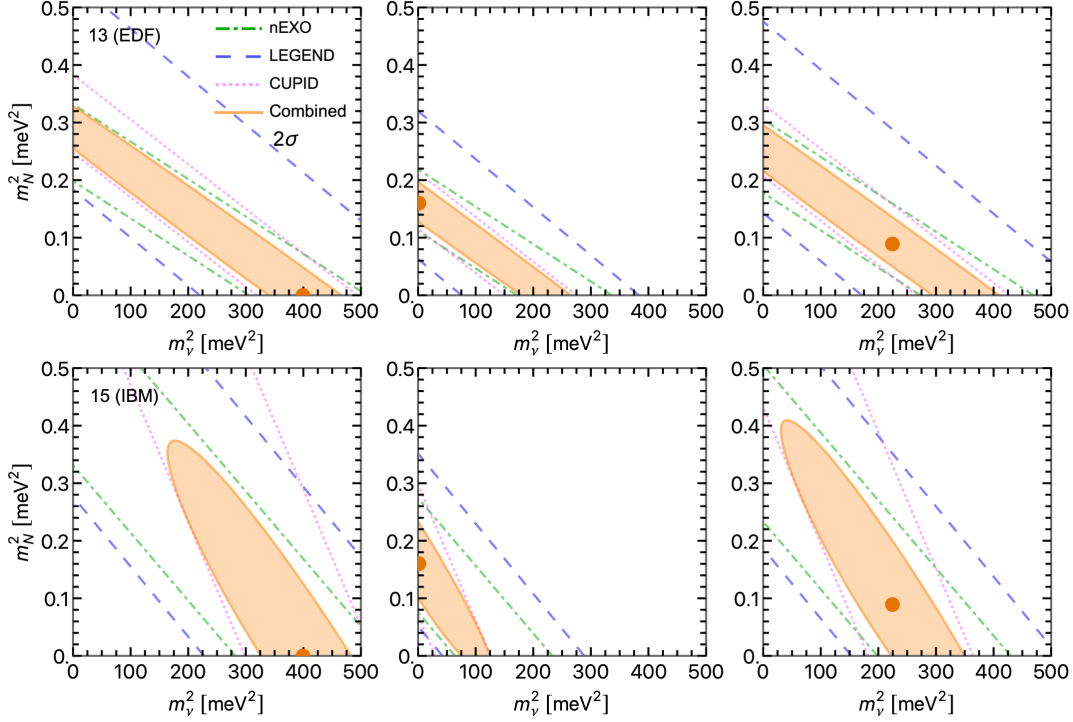


**Figure 5:** As in Fig. 4, but for the NME sets numbered as as 13 and 15 in Table 1 of [1].

demonstrate that multi-isotope searches for  $0\nu\beta\beta$  decay in ton-scale experiments have the potential to statistically distinguish between the two non-interfering mechanisms (exchange of light and heavy neutrinos) when the corresponding NME sets are well-established and exhibit significantly different ratios in at least a couple of isotopes. In the case of very similar NME ratios, the two mechanisms become degenerate.

### 3. Conclusions

We studied the  $0\nu\beta\beta$  phenomenology, when it is mediated by non-interfering exchanges of light and heavy Majorana neutrinos. The analysis incorporates current experimental data from KamLAND-Zen, EXO, GERDA, MAJORANA, and CUORE as well as prospective signals from ton-scale projects such as nEXO, LEGEND, and CUPID. We emphasized the significance of NME ratios in determining whether the mechanisms are degenerate or non-degenerate. and we derived upper bounds on the effective Majorana mass parameters from current experiments. We explored various representative cases leading to prospective  $> 3\sigma$  signals in ton-scale experiments, showing the allowed regions in the  $(m_\nu^2, m_N^2)$  parameter space.

### References

- [1] E. Lisi, A. Marrone and N. Nath, “Interplay between noninterfering neutrino exchange mechanisms and nuclear matrix elements in  $0\nu\beta\beta$  decay,” Phys. Rev. D **108** (2023) no.5, 055023 doi:10.1103/PhysRevD.108.055023 [arXiv:2306.07671 [hep-ph]].